Int J Thermophys (2007) 28:1255–1268
DOI 10.1007/s10765-007-0254-3

Thermal-Conductivity and Thermal-Diffusivity Measurements of Nanofluids by 3ω Method and Mechanism Analysis of Heat Transport

Z. L. Wang · D. W. Tang · S. Liu · X. H. Zheng · N. Araki

Received: 12 September 2006 / Accepted: 10 August 2007 / Published online: 11 September 2007

Abstract A 3ω technique is developed for simultaneous determination of the thermal conductivity and thermal diffusivity of nanofluids. The 3ω measuring system is established, in which a conductive wire is used as both heater and sensor. At first, the system is calibrated using water with known thermophysical properties. Then, the thermal conductivity and thermal diffusivity of TiO_2/distilled water nanofluids at different temperatures and volume fractions and the thermal conductivity of SiO_2 nanofluids with different carrier fluids (water, ethanol, and EG) are determined. The results show that the working temperature and the carrier fluid play important roles in the enhancement of thermal transport in nanofluids. These results agree with the predictions for the temperature dependence effect by the Brownian motion model and the micro-convection model. For SiO_2 nanofluids, the thermal-conductance enhancement becomes strong with a decrease in the heat capacity of the carrier fluids. Finally, according to our results and mechanism analysis, a corrected term is introduced to the Brownian motion model for providing better prediction of heat transport performance in nanofluids.

Keywords 3ω method · Brownian motion · Micro-convection · Nanofluids · Thermal conductivity · Thermal diffusivity

Z. L. Wang · D. W. Tang (✉) · S. Liu · X. H. Zheng
Institute of Engineering Thermophysics, Chinese Academy of Sciences, Beijing 100080, China
e-mail: dwtang@mail.etp.ac.cn

N. Araki
Department of Mechanical Engineering, Shizuoka University, Hamamatsu 432-8561, Japan

1 Introduction

Nanofluids, i.e., fluid suspensions of nanometer-sized solid particles and fibers, have been proposed as candidates for surpassing the performance of heat transfer liquids currently available. Recent experiments indicated that, compared with liquids not containing nanoparticles or containing larger particles, nanofluids show significant increases in thermal conductivity, a strong temperature dependence of the thermal conductivity, and significant increases in the critical heat flux in boiling heat transfer [1].

The transient hot-wire method (THW) has been widely used for measurements of thermal conductivities of fluids as well as nanofluids [2–4]. In practical applications, however, the method requires the attainment of very high precision of the measurement of the absolute temperature rise with time. The finite length and heat capacity of the hot wire, the finite size of the container, and possibly natural convection effects are examples of possible deviations of any realistic system from the one used in deriving the principle [2]; the experimental time should be limited. If the time is too long, the temperature difference between the hot wire and the sample fluid increases and free convection takes place which may result in significant error [4]. Additionally, this method is rather difficult to apply to electrically conducting or highly corrosive fluids because the rather long wire must be insulated with anti-corrosive and electrically insulating coatings. These disadvantages could be much reduced if the long hot wire is replaced by a much shorter wire and the measurements are taken in the frequency domain rather than in the time domain.

The 3ω method [5–7] offers a more convenient way to realize thermal transport inside a small sample. The sample is heated by an ac current, and the temperature can be deduced from the third harmonic voltage across the heater. The ac lock-in technique in the 3ω method can be sufficient to overcome the opposing effects in the THW method between a fast response and high sensitivity. An extremely small sample size as well as space-resolvable measurement are possible in characterizing the thermal conductivity of a small sample, due to the very small size of the heater compared to the long hot wire in the THW method. More importantly, the faster time window adopted also largely suppresses the interference from convection, for which the effect decreases with frequency.

The use of nanofluids in heat exchangers, especially in micro-cooling systems, may result in energy and cost savings and should facilitate the trend of device minituarization. Some new assessments and mathematical models have been proposed to analyze the thermal enhancement mechanism. Xuan and Li [8] summarized previous experimental results and concluded that the effective thermal conductivity is a function of the thermal conductivities of both the nano-material and carrier fluid, in terms of particle volume fraction, distribution, surface area, and shape. Possible explanations for the divergence between theory and experiment were suggested and explored by Keblinski et al. [9]. Jang and Choi [10] suggested an effective thermal conductivity model considering the particles' Brownian motion, focusing on the heat transfer between particles and the carrier fluid, neglecting the micro-convection mixing due to random particle motion. A potentially important development in the nanofluids field has been the recent observation by Das et al. [11] of strong temperature effects. Their

studies of Al_2O_3 nanoparticles in water have shown a two- to four-fold increase in thermal-conductance enhancement over a small temperature range, 20–50°C. Eastman et al. [12] also pointed out recently that the temperature might be important. Koo and Kleinstreuer [13] proposed a new thermal-conductivity model for nanofluids, which considers the effects of particle size, volume fraction, and temperature dependence as well as the properties of the base fluid and particle phase by considering the surrounding liquid traveling with randomly moving nanoparticles. Recently, Ren et al. [14] have proposed a theoretical model to account for the thermal-conductance enhancement including the considerations of an interfacial nano-layer formed by the liquid molecules and of micro-convection caused by the thermal motion of nanoparticles. But few studies have examined the behavior of nanofluids other than at room temperature. More studies are needed to determine the extent of such temperature-dependent performance and to provide important insights that will allow determination of the importance of particle motion in controlling thermal transport behavior.

In our view, there are about four possible reasons for the anomalously enhanced effective thermal conductivity, which can be classified as follows: the properties of nanoparticles (size, thermal conductivity, and volume fraction); the micro-convection and Brownian motion especially at high temperatures; the properties of the carrier fluid, such as thermal conductivity and heat capacity; and the aggregation of nanoparticles. In the present paper, first we describe the principle of the 3ω method for liquid thermal property measurements. Then, we report measurements of the thermal conductivity and heat capacity of TiO_2/water suspensions at different temperatures (18–65°C) and SiO_2 nanoparticle suspensions in different base fluids (water, ethanol, and EG) using the 3ω method. Finally, the Brownian model by Koo [13] and the micro-convection model by Ren et al. [14] are chosen to provide theoretical predictions of the effective thermal conductivity. The effects on heat transport due to the temperature dependence and the carrier fluid are investigated with the combination of experimental results and the two models.

2 Measuring Principle of 3ω Technique

Consider a fine-wire conductor suspended in a liquid sample serving simultaneously as a heater and as a thermometer. A sinusoidal current drives the wire at a frequency ω leading to Joule heating with a 2ω component. The magnitude and phase of the resulting temperature rise at 2ω depend on the thermal resistance pertaining to the thermal conductivity and thermal capacity of the wire. Due to the linear temperature dependence of the electrical resistance (with a temperature coefficient of resistance, α), the resistance of the wire is modulated at 2ω. Consequently, the current at ω mixed with the resistance at 2ω leads to a voltage signal at 3ω, which yields information on the thermophysical properties of the wire and surrounding liquid. When a sinusoidal current at ω with a dc offset is supplied, the voltage response occurs at dc and three harmonics in the form [15]:

$$U(t) = U_{\mathrm{dc}} + U_{1\omega}(t) + U_{2\omega}(t) + U_{3\omega}(t) \tag{1}$$

Equation 1 can also be expressed in terms of rms quantities as usually measured by a lock-in amplifier:

$$U_{n\omega,\mathrm{rms}} = 2\alpha R^2 I^3(\mathrm{X}_n + i\,\mathrm{Y}_n) \tag{2}$$

where X_n and Y_n are functions of the nth-harmonic with $n=0$, 1, 2, 3, containing valuable information on thermophysical properties. Therefore, the various harmonic signals can be used to determine the properties. Here, the third harmonic signal is especially valuable because it contains information on the thermal conductivity and heat capacity. When a sinusoidal current at frequency ω without a dc offset is supplied, the voltage across the heater is

$$U(t) = R_0 I\cos(\omega t) + \frac{R_0\alpha I\theta}{2}\cos(\omega t+\varphi) + \frac{R_0\alpha I\theta}{2}\cos(3\omega t+\varphi) \tag{3}$$

where R_0 is the resistance of the heater at the initial temperature, I is the ac current amplitude, θ is the temperature oscillation amplitude of the heater, and φ is the phase shift between the electrical signal and thermal response signal.

For the experimental setup used here, the heater, a Pt wire of length l and radius r_0, is immersed in an isotropic nanofluid and initially kept at thermal equilibrium with the surrounding liquid. An ac current signal $I = I_0\sin(\omega t)$ is applied to the wire, then the power per unit volume Q is generated in the wire. For the case of $l \gg r_0$, the temperature oscillation in the axial direction is uniform and the heat transfer by natural convection of nanofluids is negligible. The temperature oscillations in the frequency domain in the Pt wire and nanofluids are expressed as follows: In the Pt wire,

$$\frac{\mathrm{d}^2\theta_1}{\mathrm{d}r^2} + \frac{1}{r}\frac{\mathrm{d}\theta_1}{\mathrm{d}r} - \mathrm{i}2\omega\theta_1/a_1 = -\frac{Q}{\lambda_1} \tag{4}$$

In the nanofluid,

$$\frac{\mathrm{d}^2\theta_2}{\mathrm{d}r^2} + \frac{1}{r}\frac{\mathrm{d}\theta_2}{\mathrm{d}r} - \mathrm{i}2\omega\theta_2/a_2 = 0 \tag{5}$$

The corresponding boundary conditions at $r = r_0$

$$\theta_1 = \theta_2, \quad \lambda_1\frac{\mathrm{d}\theta_1}{\mathrm{d}r} = \lambda_2\frac{\mathrm{d}\theta_2}{\mathrm{d}r}$$

Considering the natural boundary conditions, the solutions in the frequency domain are

$$\theta_1 = \frac{Q\lambda_2 q_2 K_1(q_2 r)}{\lambda_1 q_1^2\Delta} \tag{6}$$

$$\theta_2 = \frac{Q\lambda_1 q_1 I_1(q_1 r)}{\lambda_1 q_1^2\Delta} \tag{7}$$

$$\Delta = \lambda_1 q_1 I_1(q_1 r_0) K_0(q_2 r_0) + \lambda_2 q_2 I_0(q_1 r_0) K_1(q_2 r_0) \tag{8}$$

where $q_1 = (\mathrm{i}2\omega/a_1)^{1/2}$ and $q_2 = (\mathrm{i}2\omega/a_2)^{1/2}$. $|q_1|^{-1}$ and $|q_2|^{-1}$ are the thermal penetration lengths along the axial direction in the Pt wire and nanofluid, respectively. λ_1 and λ_2 are the thermal conductivities of the Pt wire and liquid, respectively. a_1 and a_2 are the thermal diffusivities of the Pt wire and liquid, respectively. I_0, K_0, I_1, and K_1 are the zeroth-order and first-order modified Bessel functions.

For the case of an electrically conductive liquid, an insulating layer with a thickness of several micrometers is coated on the Pt wire, which only introduces a temperature drop independent of frequency. Therefore, the temperature drop of the insulating coating can be accurately determined by Fourier's law to modify the measured temperature oscillations of the Pt wire, provided the heating power Q and thermal conductivity of the insulating coating are known.

For measurements of the thermal conductivity of a liquid by the 3ω method, the temperature oscillation amplitude changes could be very small in the radial direction in the Pt wire due to the very low heating power by the ac signal and the large thermal conductivity of the Pt wire. Therefore, it is reasonable to substitute the temperature oscillation amplitude, $\theta_1(\omega, r_0)$ or $\theta_2(\omega, r_0)$, on the surface of the Pt wire for the average value of the temperature oscillation amplitude across the Pt wire in the radial direction. At low frequency, the thermal penetration length in the Pt wire is much larger than r_0, and

$$\theta_2(\omega, r_0) = \frac{Q r_0^2}{2\lambda_2 q_2 r_0 K_1(q_2 r_0)/K_0(q_2 r_0) + \lambda_1 (q_1 r_0)^2} \tag{9}$$

According to the characteristics of Bessel functions, if the variable is very small and the heat capacity of the Pt wire is negligible, K_0 and K_1 can be replaced by

$$K_0(z) \approx -\ln z + \ln 2 - \gamma$$
$$K_1(z) \approx -K_0(z) = 1/z$$

where z is a complex variable, γ is Euler's constant, and P is the heating power across the Pt wire. Equation 9 can be simplified as

$$\theta_2(\omega, r_0) = \frac{P}{2\pi\lambda_2 l}\left[-\ln|q_2 r_0| + \ln 2 - \gamma - \mathrm{i}\pi/2\right] \tag{10}$$

According to Eqs. 3 and 9 or 10, the relationship between the temperature oscillation amplitude and the third harmonic component can be derived as

$$\theta_2(\omega, r_0) = \frac{2}{\alpha}\frac{U_{3\omega}}{U_{1\omega}} \tag{11}$$

where $U_{3\omega}$ and $U_{1\omega}$ are voltages detected by the lock-in amplifier at 3ω and 1ω, respectively.

Further analysis of Eqs. 9 and 10 shows that the thermal conductivity of a liquid has more effect on the temperature oscillation amplitude or the third harmonic voltages than does the thermal diffusivity of the liquid. It is clear from Eq. 10 that there exists a linear relationship between the temperature oscillation amplitude and the logarithmic frequency at low frequency. Therefore, the thermal conductivity of a liquid can be obtained directly from Eq. 10 and the real part of the measured temperature oscillation amplitudes. The thermal diffusivity can be obtained by extending the frequency band to a value higher than 1 kHz. Then, the thermal diffusivity is determined by fitting the measured data to either Eqs. 6 or 7 at high frequency. At low frequency, the effects of the properties' uncertainties of the Pt wire on the thermal conductivity of the liquid are negligible. The uncertainty of the measured thermal conductivity of nanofluids mainly arises from the uncertainty of the temperature coefficient of the Pt wire resistance and is estimated to be within $\pm 1.5\%$. At high frequency, the uncertainty of the measured thermal diffusivity of nanofluids arises mainly from the uncertainties of the properties of the Pt wire, the temperature coefficient of the Pt wire resistance, and the thermal conductivity obtained at low frequency. The total uncertainty of the measured thermal diffusivities of nanofluids is estimated to be within $\pm 6.5\%$.

3 Experimental Setup and Conditions

The block diagram of our measurement system is given in Fig. 1. A digital lock-in amplifier (Model 7280) is used to measure the 1ω and 3ω signals. Due to the finite dynamic reserve of the lock-in, it is necessary to eliminate the 1ω voltage before the 3ω voltage is measured. The subtraction is accomplished using an analog balance bridge circuit. A function generator is chosen as a voltage source in most traditional 3ω measurements. A set of circuits with low noise has been built. The signals from the wire sample and potentiometer are fed into two unit-gain differential amplifiers U1 and U2, respectively. The potentiometer is adjusted to balance the first harmonic voltage signal to that across the wire sample. The differential input to the lock-in amplifier can then reduce the 1ω component to an acceptable level. Other experimental details include turning off all line filters to keep from distorting 1ω and 3ω signals over the typical frequency range of 1–100 Hz.

The Pt wire immersed in the nanofluid sample has a length of 8 mm between the two central pads and a diameter of 17 μm. The volume of the cylindrical container with an inner diameter of 16 mm is about 8 mL. The thermal penetration length will be less than hundreds of micrometers, due to the relatively low thermal conductivity of nanofluids at low frequency. Therefore, the boundary conditions of the infinite size for heat conduction equations in the frequency domain can be satisfied even for a liquid sample with a rather small volume. The container is placed in a water heating chamber to minimize the temperature fluctuations of nanofluids. The Pt wire and the four lead pad joints are well insulated by depositing a 50 nm-thick SiO_2 layer; the inner wall of the container is coated with anti-static material so as to eliminate the influence of the electric field on the nanoparticles.

Figure 2 shows the measured real part of the temperature oscillation amplitude for distilled water and TiO_2 + distilled water nanofluids at a volume fraction of 4% at

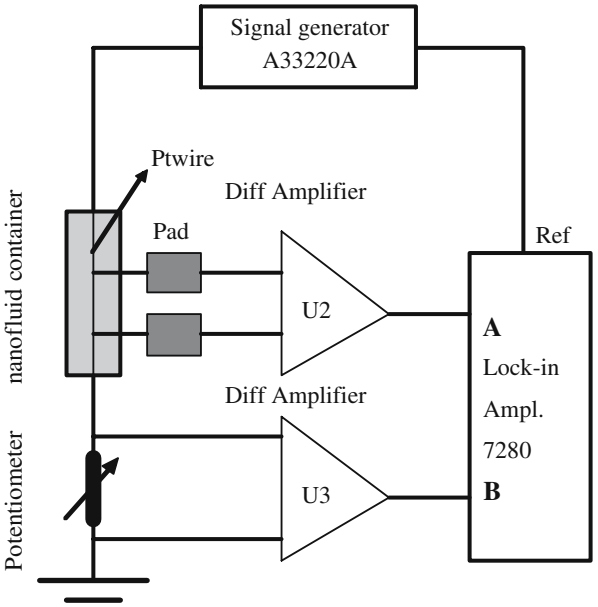

Fig. 1 Measurement system for 3ω method

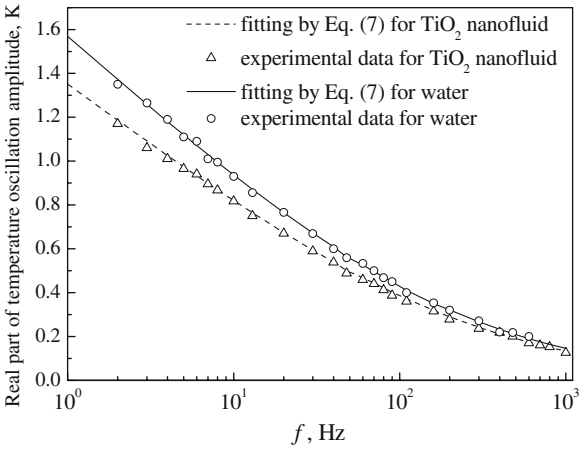

Fig. 2 Real part of temperature oscillation amplitude

20°C. The symbols are experimental data, and the solid and dashed lines are fitted results using either Eq. 6 or 7 at $r = r_0$. Clearly, there exists a linear section on the temperature oscillation amplitude and the logarithmic frequency curve at low frequency below 15 Hz. Also, the experimental data agree well with the solution of the heat-conduction equation in the frequency domain, which confirms that the 3ω method can be used to realize a reduction in the effect of natural convection.

Table 1 Properties of test materials for preparing nanofuids (20°C)

	TiO_2	SiO_2	Distilled water	Ethanol	Ethylene glycol
Specific gravity	4	2.22	1	0.789	1.111
Thermal conductivity ($W \cdot m^{-1} \cdot K^{-1}$)	11.9	1.38	0.625	0.169	0.252
Specific heat ($J \cdot g^{-1}$)	0.7	0.73	4.18	2.5	2.72
Average size (nm)	26	23	–	–	–

4 Results and Mechanism Analysis

First, the measurement system using the 3ω technique is calibrated using distilled water at 20°C. The measured data are presented in Fig. 2. As mentioned above, there exists a linear section with a constant slope for the curve of temperature oscillation amplitude versus logarithmic frequency at low frequency. According to Eq. 10, the measured data at 5 and 10 Hz are used to determine the thermal conductivity of distilled water, $0.58\,W \cdot m^{-1} \cdot K^{-1}$. Then the data at frequencies higher than 30 Hz are fitted using Eq. 6 to obtain the thermal diffusivity of distilled water, $1.37 \times 10^{-7}\,m^2 \cdot s^{-1}$, and the calculated heat capacity is $4.24\,MJ \cdot m^{-3} \cdot K^{-1}$. These results are close to the data in Table 1, which demonstrates the reliability of the measurement system.

In the present experiment, the nanofluids are prepared with the conventional two-step method used by most researchers. The properties of the test material are shown in Table 1. Figures 3 and 4 show the temperature-dependent characteristics of the thermal-conductivity and thermal-diffusivity enhancement, respectively, at volume fractions of 1%, 2%, and 4% for TiO_2 + distilled water nanofluids measured from 18 to 65°C. Figure 5 shows the thermal-conductivity enhancement of SiO_2 + distilled water, EG, and ethanol nanofluids at a volume fraction of 1% at 20°C. In the following analysis, the thermal-conductivity enhancement β is defined as

$$\beta = (\lambda_{\text{eff}} - \lambda_{\text{f}})/\lambda_{\text{f}} \times 100\% \tag{12}$$

and the thermal-diffusivity enhancement η,

$$\eta = (a_{\text{eff}} - a_{\text{f}})/a_{\text{f}} \times 100\% \tag{13}$$

where λ_{eff} and a_{eff} are the effective thermal conductivity and effective thermal diffusivity of the nanofluids, and λ_{f} and a_{f} are the effective thermal conductivity and effective thermal diffusivity of the carrier fluids, respectively.

4.1 Carrier Fluid's Heat-Capacity Dependence of Thermal-Conductivity Enhancement

Up to now, there has been numerous reports on the effect of nanoparticles' properties (size, shape, volume fraction, etc.) and the thermal conductivity of carrier fluids

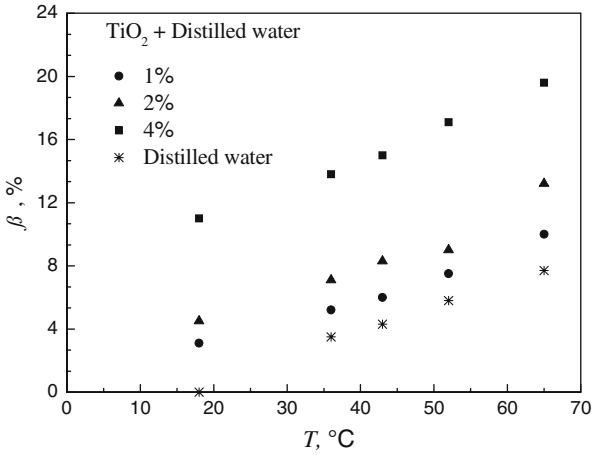

Fig. 3 Temperature dependence of thermal-conductivity enhancement for different volume fractions

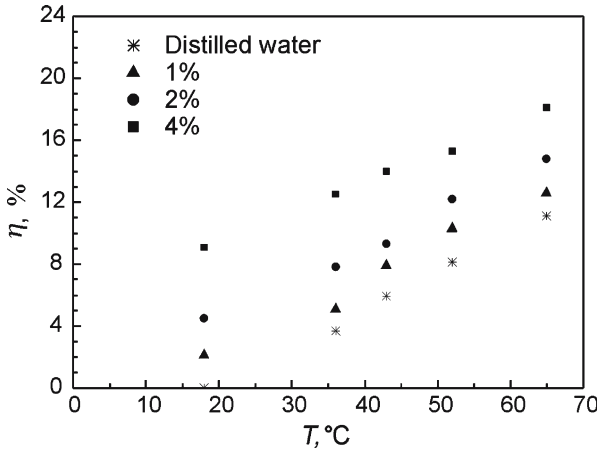

Fig. 4 Temperature dependence of thermal-diffusivity enhancement for different volume fractions

on the thermal-conductivity enhancement of nanofluids, but reports on the effect of the temperature dependence and heat capacity of the carrier fluid are seldom found in the literature. Recently, Koo and Kleinstreuer [13] proposed a new model with consideration of the particle Brownian motion as

$$\lambda_{\text{eff}} = \lambda_{\text{static}} + \lambda_{\text{Brownian}} \tag{14}$$

$$\lambda_{\text{Brownian}} = 5 \times 10^4 \varepsilon \phi C_{\text{f}} \sqrt{\frac{kT}{\rho_d D}} G(T, \phi, \text{etc.}) \tag{15}$$

where λ_{static} (calculated by the Maxwell model) and $\lambda_{\text{Brownian}}$ are the thermal conductivities of the static dilute suspension and the enhancement due to Brownian motion,

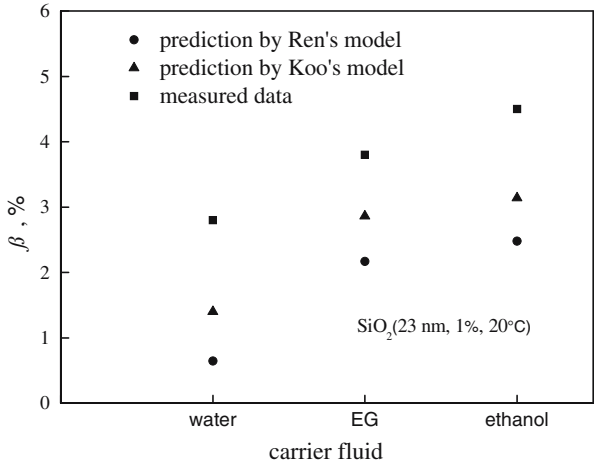

Fig. 5 Thermal-conductivity enhancement for different carrier fluids at a volume fraction of 1%

ε represents the fraction of the liquid volume traveling with a particle, ϕ is the volume fraction, C_f is the heat capacity of the carrier fluid, k is the Boltzmann constant, T is the temperature of the nanofluids, ρ_d is the density of the nanoparticles, and G is a function of the temperature and volume fraction, depending on the properties of the intervening fluid and particle interactions. According to Koo' s analysis, for the case of a small volume fraction, $\phi < 1\%$, where the particle interaction effect is relatively less significant due to both the long interparticle distance and potential retardation effect, the function ε is independent of the type of particle and takes the form,

$$\varepsilon = 0.0137(100\phi)^{-0.8229} \tag{16}$$

On the basis of Gupte's numerical results of micro-convection in a unit cell [17], Ren et al. [14] presented a model for the effective thermal conductivity with consideration of micro-convection,

$$\lambda_{\text{eff}} = \lambda_f \left[1 + F(Pe) + 3\Theta\phi_T + \frac{3\Theta^2\phi_T^2}{1 - \Theta\phi_T} \right] \tag{17}$$

where F is a function of the modified Peclet number pertaining to the mean motion velocity of the nanoparticles and the thermal diffusivity of the carrier fluid, ϕ_T is the total volume fraction of the nanoparticles and nano-layers, and Θ is a function of the thermal conductivities of the nanoparticles and carrier fluid. Equation 17 relates the thermal-conductivity enhancement of a nanofluid to the system properties such as the thermal-conductivity of the carrier fluid and nanoparticles, the volume fraction, the thickness of the nano-layers, and the temperature.

For the three different carrier fluids (distilled water, EG, and ethanol) for SiO_2 nanoparticle suspensions at 1%, the heat capacities are 4.18, 3.022, and 1.973 $\text{MJ} \cdot \text{m}^{-3} \cdot \text{K}^{-1}$, respectively. The ratios of the thermal-conductivity enhancement among the three

suspensions are 0.26:0.88:1 by Ren's model, 0.44:0.91:1 by Koo's model, and 0.62:0.84:1 for the experimental data, which are also explained in the corresponding observations in Fig. 5 and justifies the effect of the micro-convection enhancement mechanism due to Brownian motion. The heat-capacity behavior of the nanofluids, confirmed using SiO_2 nanoparticle suspensions, is in agreement with the experimental result of Xie et al. [16] for a nanofluid of Al_2O_3. This behavior can also be explained using the unit cell physical model of Gupte and Advani [17] to determine the temperature distribution and heat flux through the carrier fluid with induced micro-convection. For a given temperature gradient across the boundaries of the unit cell, the larger the heat capacity of the carrier fluid, the smaller the modified Peclet number, the smaller the heat flux through the unit cell, and then a smaller effective thermal-conductivity enhancement is obtained.

4.2 Temperature Dependence of Thermal-Conductivity Enhancement

Both Eqs. 15 and 17 suggest that the thermal motion of nanoparticles should show a temperature dependence; it is expected that the thermal-conductivity of a nanofluid will vary significantly with temperature. The present experimental results in Fig. 3 confirm that the thermal-conductivity enhancement increases with temperature, and an 11% enhancement is observed for TiO_2 + distilled water nanofluids at a volume fraction of 4% compared to distilled water at the same temperature. An enhancement of up to 19.6% is observed at 4% and 65°C compared to distilled water at 18°C, for which an enhancement of 8% is due to distilled water. Further comparisons of the experimental results with the two models are presented in Figs. 6 and 7. For TiO_2 + distilled water nanofluids at different volume fractions, Fig. 6 shows comparisons of the present data with results of Pak and Cho [18] (size of TiO_2 nanoparticle, 27 nm) and the predictive results by Ren's and Koo's models at 18°C, and Fig. 7 shows comparisons at 65°C. The deviations between the measured data and the predictions are small and acceptable at low temperatures and at low volume fractions (see Fig. 6) while the deviations at high temperatures are large (see Fig. 7). In fact, the temperature dependence of the thermal-conductivity enhancement by Ren's model is less than that by Koo's model, although the predicted values by the latter model are less than the measured data by about 40%. In our view, the large discrepancy in the temperature dependence between the experimental and theoretical results can be probably attributed to two factors: one is that the volume of the carrier fluid is disturbed by the micro-convection effect and transport with the nanoparticles has been underestimated; the other is that there are not many data sets available for determining the temperature dependence of properties of the intervening fluid and particle interactions.

Since both Koo's and Ren's models underestimated the temperature dependence of the thermal-conductivity enhancement, we try to introduce a correction term to Koo's model. There are still some uncertainties in the derivation process for Koo's model, such as the determination of the average traveling distance of a nanoparticle without changing its direction and the functions, ε and G. All the uncertainties may be relative to the temperature increase; for the experimental conditions, $1\% < \phi < 4\%$ and

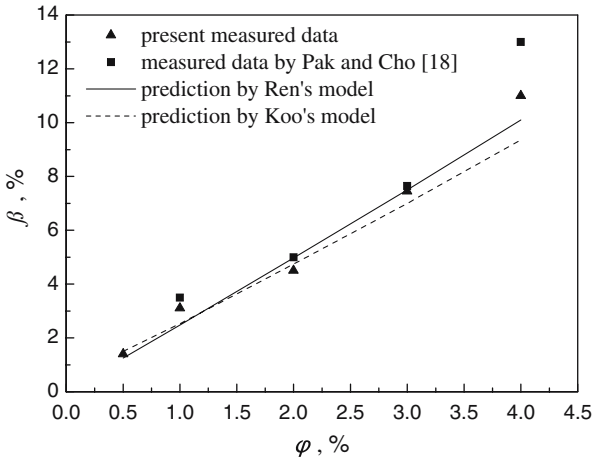

Fig. 6 Comparisons between the measured and predicted results at 18°C

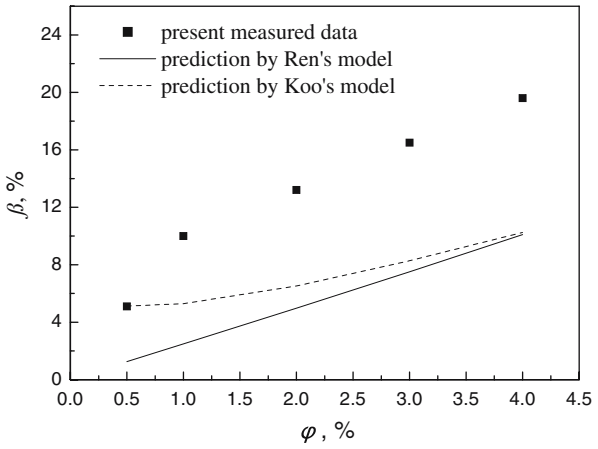

Fig. 7 Comparisons between the measured and predicted results at 65°C

$291\,\mathrm{K} < T < 338\,\mathrm{K}$, we introduce an exponential function of temperature into Koo' model,

$$\lambda_{\text{Brownian}} = 5 \times 10^4 \varepsilon \phi C_{\text{f}} \sqrt{\frac{kT}{\rho_d D}} G(T, \phi, \text{etc.}) \left(\frac{T}{273}\right)^{2.5} \tag{18}$$

Comparisons between the experimental data and the predicted results by Eq. 18 are presented in Fig. 8. The maximum discrepancy is reduced to less than 5% by introducing a correction term to Koo's model. Additional experimental data are desired to have a deeper insight into the mechanism of the temperature-dependent enhancement.

In short, a strong temperature dependence is observed and confirmed by the present experimental results for TiO_2 + distilled water nanofluids at volume fractions up to 4% over the temperature range, 18 to 65°C, which shows about a two-fold increase in the

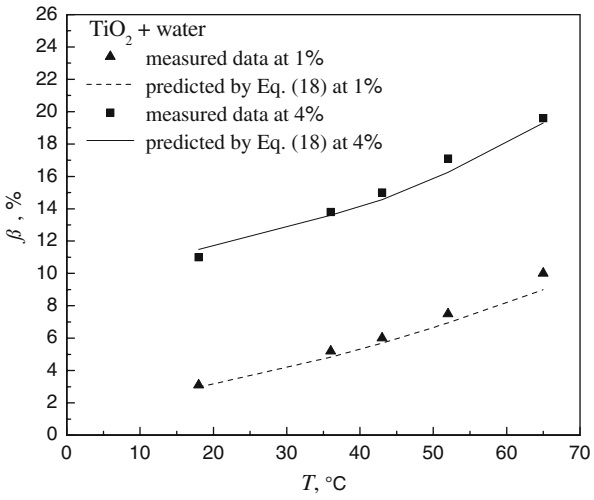

Fig. 8 Comparisons between experimental data and predicted results

thermal-conductivity enhancement. Furthermore, if this behavior occurs over a wide temperature range, it could make nanofluids particularly attractive for applications at elevated temperatures. As has been stated by Eastman et al. [12], the temperature dependence will open up the possibility that nanofluids could be employed as "smart fluids," sensing hot spots and providing more rapid cooling in micro-cooling systems and mini-heat exchangers.

5 Conclusions

(1) The 3ω experimental method is established to simultaneously measure the thermal conductivity and thermal diffusivity of liquid samples. The fast and accurate third harmonic signals can be detected by a lock-in amplifier in a long time and wide frequency band, compared to the THW method. The method has the potential to characterize the thermal properties of small liquid samples (few mL, or even less) due to the small thermal penetration length at high frequency.

(2) The thermal conductivity of TiO_2/distilled water nanofluids increases with temperature, an enhancement of about 20% is observed for a volume fraction of 4% at 65°C. For SiO_2 nanoparticle suspensions at a volume fraction of 1%, the thermal-conductivity augmentation ratio increases with a decrease of the heat capacity of the carrier fluid, which is in agreement with Koo's and Ren's models.

(3) Both Koo's and Ren's models underestimate the thermal-conductivity enhancement at high temperatures; the predictions agree well with each other and the experimental data at room temperature due to the consideration of microconvection effects introduced by Brownian motion.

(4) The stability of the suspension is a crucial issue for both scientific research and practical applications. Particle aggregation and the formation of extended structures of linked nanoparticles may be responsible for much of the disagreement between experimental results and the predictions of effective medium theory.

Simultaneous studies of the temperature dependence of the thermal conductivity and viscosity of nanofluids at higher temperatures are desired and may give additional insight.

Acknowledgments The authors would like to thank Prof. L.H. Zhang of the Institute of Physics, Chinese Academy of Sciences, for solving the noise cancellation and dynamic reserve problems of the lock-in amplifier. We also thank Dr. Z.G. Liu of the Academy of Sciences, Shandong Province, for determining the temperature coefficient of resistance, and thank Dr. F. Chen of University of Houston for helpful advice on the 3ω system. The work is supported by the National Natural Science Foundation of China Grant No. 50376066.

References

1. P. Keblinski, J.A. Eastman, D.G. Cahill, Mater. Today **8**, 36 (2005)
2. J.J. Vadasz, S. Govender, P. Vadasz, Int. J. Heat Mass Transfer **48**, 2673 (2005)
3. J.A. Eastman, S.U.S. Choi, S. Li, W. Yu, L.J. Thompson, Appl. Phys. Lett. **78**, 718 (2001)
4. Y. Xuan, Q. Li, Int. J. Heat Mass Transfer **21**, 58 (2000)
5. D.G. Cahill, R.O. Pohl, Phys. Rev. B **35**, 4067 (1987)
6. D.G. Cahill, Rev. Sci. Instrum. **61**, 802 (1990)
7. T.Y. Choi, D. Poulikakos, Appl. Phys. Lett. **87**, 013108 (2005)
8. Y. Xuan, Q. Li, Int. J. Heat Fluid Flow **21**, 58 (2000)
9. P. Keblinski, S.R. Phillpot, S.U.S. Choi, J.A. Eastman, Int. J. Heat Mass Transfer **45**, 855 (2002)
10. S.P. Jang, S.U.S. Choi, Appl. Phys. Lett. **84**, 4316 (2004)
11. S.K. Das, N. Putra, P. Thiesen, W. Roetzel, ASME J. Heat Transfer **125**, 567 (2003)
12. J.A. Eastman, S.R. Phillpot, S.U.S. Choi, P. Keblinski, Annu. Rev. Mater. Res. **34**, 219 (2004)
13. J. Koo, C. Kleinstreuer, J. Nano. Res. **6**, 577 (2004)
14. Y.J. Ren, H.Q. Xie, A. Cai, J. Phys D: Appl. Phys. **38**, 3958 (2005)
15. L.R. Holland, R.C. Smith, J. Appl. Phys. **37**, 4528 (1966)
16. H.Q. Xie, J. Wang, T.G. Xi, Y. Liu, J. Appl. Phys. **91**, 4568 (2002)
17. S.K. Gupte, S.G. Advani, Int. J. Heat Mass Transfer **36**, 2495 (1995)
18. B.C. Pak, Y.I. Cho, Exp. Heat Tranfer **11**, 151 (1998)